Link-length Analysis for First-neighbor Optical ISLs in Ultra-dense LEO Constellations

Igor P. Vieira, Thiago C. Pita and Darli A. A. Mello

Abstract— In this work, we performed a detailed study of first-neighbor type connections for ultra-dense next-generation low-Earth orbit (LEO) constellations. The link lengths and their corresponding free-space path losses (FSPLs) are quantified for both intraorbital and interorbital connections (the latter in two distinct topologies). Each of the inter-satellite links (ISLs) is then categorized with respect to the minimum altitude reached, checking for eventual physical changes in the propagation medium or occlusion of the beam by the Earth's surface.

Keywords— Satellite Communications, LEO constellations, LEO-LEO, ISL.

I. INTRODUCTION

High-speed ubiquitous broadband Internet (UBI) provided by swarms of small low-Earth orbit (LEO) satellites is a promising innovation in the sector of telecommunications services. Although the technology dates back to the 1990s, with pioneering companies like Globalsat and Iridium holding constellations in non-geostationary orbits, the model viability has been contested due to prohibitive costs associated with production, launch, operation, and maintenance [1], [2]. Still, with the rapid progress in the space industry witnessed in recent years, several new players, including private companies like SpaceX, Telesat, Amazon, and OneWeb, are planning to send tens of thousands of satellites into LEO over the next decade [3], [4].

LEO constellations are typically designed to meet two chief aims: (1) low latency and (2) global connectivity. In this sense, they are composed of two or more shells, each one of them typified by a set of orbital planes with common altitude and inclination. Modern systems are characterized by the occurrence of ultra-dense orbits in medium-range inclinations (between 40° and 55°) – which is why they are sometimes referred to as "mega-constellations" –, thus concentrating their satellite footprints in the Earth's most populated regions, with only a small quota of its capacity for the polar ones. Furthermore, the number of satellites per plane is commonly a constant value across the same shell, resulting in a highly symmetrical moving grid over the globe.

LEO-LEO type connections, where each LEO satellite would correspond to a vertex in the grid [5], established via free-space optics (FSO) is the technological state-of-the-art in satellite communications, with several constellation operators signaling positively in their petitions to the Federal Communications Commission (FCC) to the implementation of optical inter-satellite links (OISLs) in their systems. Indeed, Pachler et al. [4] demonstrated, for four of the largest current LEO constellations, that the use of four OISLs per satellite is capable of increasing the total throughput between 13% and 42% for 20 Gbps optical links, subject to the constellation architecture, when compared to scenarios that decline to use them. A remarkable feature of OISLs in LEO constellations is their ever-changing length, given the relative movement between the transmitter and receiver satellite pairs. The link length evolution in these systems is dictated by a collection of constellation parameters (e.g., altitude, orbital plane inclination, phase factor, number of satellites per plane, and number of planes per shell), and reflects in free-space path losses (FSPLs), received powers and, therefore, signal-to-noise ratios (SNRs) equally time-dependent and periodic.

The potentialities and challenges associated with the new era LEO mega-constellations are gradually being identified. Although still scarce, the literature already has important contributions focused on orbital debris and collision avoidance [6], [7], [8], coverage capabilities [9], [10], and system performance analysis [3], [4]. In this work, we propose a comprehensive characterization of link lengths, and their respective FSPLs, for first-neighbor type connections, assuming architectures based on some of the largest up coming LEO commercial constellations [11]-[21]. Both intra and interorbit first-neighbor connections are assessed (the latter in two distinct topologies). We address the worst- and best-case scenarios in the condition when some of the constellation parameters are not publicly available (namely, the phase factor). Besides analyzing the link length excursion, we also consider the minimum altitude of the link, categorizing it with respect to the lowest atmospheric layer reached and checking for potential occlusions by the Earth's surface.

The rest of the paper is organized as follows. In Sec. II, the LEO architectures are described. In Sec. III, the Walker model is presented and the patterns of connections with first neighbors are defined. In Sec. IV, the entire characterization regarding first-neighbor OISLs is performed. Finally, Sec. V concludes the paper.

Igor P. Vieira and Thiago C. Pita are with the School of Electrical and Computer Engineering (FEEC), University of Campinas (UNICAMP), Campinas-SP, 13083-852, BR, e-mail: i217002@dac.unicamp.br, t234633@dac.unicamp.br; Darli A. A. Mello is with the Department of Communications (DECOM), School of Electrical and Computer Engineering (FEEC), University of Campinas (UNICAMP), Campinas-SP, 13083-852, BR, e-mail: darli@unicamp.br.

II. ORBIT CHARACTERISTICS FOR COMMERCIAL LEO CONSTELLATIONS

The largest LEO systems for broadband services, labeled here from **A** to **D**, are in different stages of maturity. Thus, in order to guarantee a common basis of comparison between

them, the architectures are assumed in their final versions (full deployments), as described in their FCC fillings as of January 2021 [4]. Table I presents a summary of the orbit characteristics, including altitude (H), inclination (θ), number of orbital planes per shell (P), number of satellites per plane (S), and total number of satellites in the constellation (N). As can be seen, there is no pattern in the choice of orbit characteristics among the different constellations. System **B**, which has the largest number of satellites, was the only one to keep all shells at the same altitude ($H = 1,200$ km). System **D**, in turn, is characterized by square shells, in which the number of orbital planes is always equal to the number of satellites per plane. With the exception of the system **D**, which concentrates all its shells in medium inclinations, all the others allocate 10% to 30% of their total satellites in polar orbits. The satellites' orbital periods, solely dependent on the altitude of the shells, vary between about 95 min (for $C^{(1)}$, at 540 km) and 112 min (for $A^{(2)}$, at $1,325$ km).

TABLE I

ORBIT CHARACTERISTICS OF FULLY DEPLOYED LEO CONSTELLATIONS. $Q^{(m)}$ STANDS FOR THE m-TH SHELL OF THE SYSTEM $\mathbf{Q} \in \{\mathbf{A}, \mathbf{B}, \mathbf{C}, \mathbf{D}\}$.

System	Shell	H [km]	θ [°]	P	S	N
A	$A^{(1)}$	1,015	98.98	27	13	1,671
	$A^{(2)}$	1,325	50.88	40	33	
B	$B^{(1)}$	1,200	87.9	36	49	6,372
	$B^{(2)}$	1,200	55	32	72	
	$B^{(3)}$	1,200	40	32	72	
C	$C^{(1)}$	540	53.2	72	22	4,408
	$C^{(2)}$	550	53	72	22	
	$C^{(3)}$	560	97.6	6	58	
	$C^{(4)}$	560	97.6	4	43	
	$C^{(5)}$	570	70	36	20	
D	$D^{(1)}$	590	33	28	28	3,236
	$D^{(2)}$	610	42	36	36	
	$D^{(3)}$	630	51.9	34	34	

III. FIRST-NEIGHBOR CONNECTIONS

The Walker constellation model (WCM) [22], illustrated in Fig. 1, distributes evenly a total of N satellites throughout P circular orbital planes of same inclination and altitude. Thus each component of the position vector, $r_{ik} \equiv x_{ik}\hat{i} + y_{ik}\hat{j} + z_{ik}\hat{k}$, of the k-th satellite in the i-th orbital plane, is described by

$$\begin{bmatrix} x_{ik} \\ y_{ik} \\ z_{ik} \end{bmatrix} \equiv R \begin{bmatrix} \cos\theta \sin\rho \sin\Omega(t) + \cos\rho \cos\Omega(t) \\ \cos\theta \cos\rho \sin\Omega(t) + \sin\rho \cos\Omega(t) \\ \sin\theta \sin\Omega(t) \end{bmatrix}, \quad (1)$$

where R is the sum of the constellation's altitude, H, with the Earth's radius, $R_{\oplus} \approx 6.371$ km, $i \in [0, P-1]$ and $k \in [0, S-1]$, $j, k \in \mathbb{N}$. Here,

$$\rho \equiv \left(\frac{2\pi i}{P}\right) \quad \text{and} \quad \Omega(t) \equiv \omega t + 2\pi \left(\frac{k}{S} + \frac{iF}{PS}\right),$$
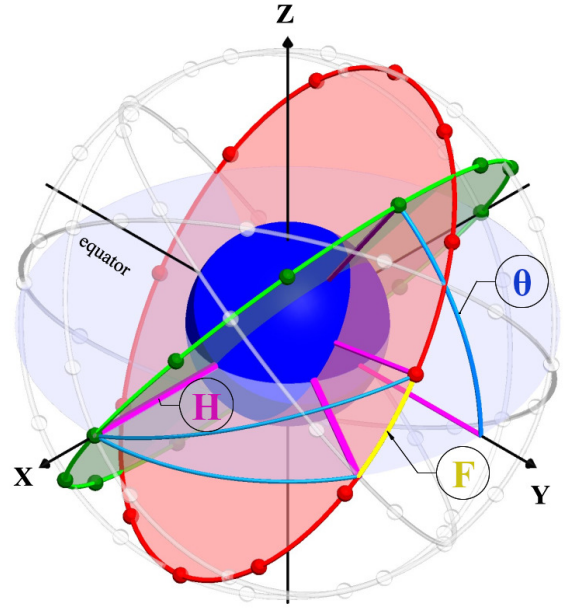

Fig. 1. WCM parameters. Two adjacent planes highlighted (in red and green colors). The small spheres evenly distributed along these planes represent the satellites. H denotes the constellation's altitude with respect to the Earth's surface, θ is the orbital plane's inclination angle, and F is the phase factor.

where $F \in [0, P-1]$ is the phase factor, ω is the satellites' flight velocity, and t is the time.

Typically, each satellite establishes four OISLs with its first neighbors: two of intraorbital nature – connecting k-to-$k+1$ and k-to-$k-1$ satellites in the same orbital plane –, two of interorbital nature – connecting k-to-k or k-to-$k-1$ in adjacent planes. Interorbital OISLs appear in red in Fig. 2a (k-to-k) and in green in Fig. 2b (k-to-$k-1$), while all intraorbital OISLs, in both diagrams, are depicted in black.

IV. LINK LENGTH AND FSPL FOR OISLs

The link length can be obtained for any OISLs by assigning a pair of first-neighbor satellites in Eq. (1) and computing the norm of the relative position vector between them. However, to the best of our knowledge, the phase factor values for the architectures listed in Table I is not publicly available in their FCC petitions nor can be found in the literature. It should be noted that the phase factor is an important parameter for interobital connections as it determines the relative angular offset between satellites in adjacent planes. In view of this, all the values of F that promote the shortest and largest link lengths for the two interorbital topologies are considered, addressing, in so doing, the best and worst-case scenarios, respectively.

Table II presents the relative distances between the emitter and receiver pairs, the corresponding FSPLs, as well as the lowest atmospheric layer reached by the beam. All quantities with bar (e.g., $\bar{L}$ and $\bar{r}$) refer to intraorbital connections, while those with hat (e.g., $\hat{L}_{\min}$, $\hat{r}_{\min}$, $\hat{F}_{\min}$) and with tilde (e.g., $\tilde{L}_{\min}$, $\tilde{r}_{\min}$, $\tilde{F}_{\min}$) refer to interorbital k-to-k and k-to-$k-1$ connections, respectively. Notations used without these indicators (e.g., L and r) are summarily applicable to any type
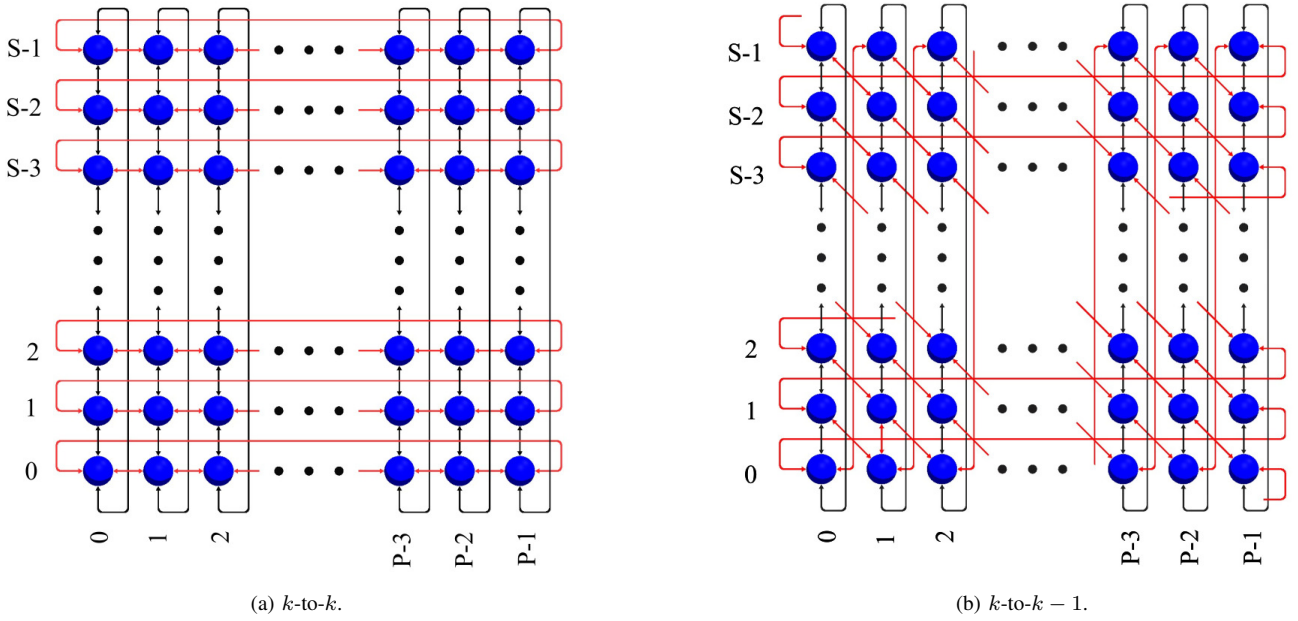
(a) k-to-k.

(b) k-to-$k-1$.

Fig. 2. First-neighbor connection patterns (illustrated for $F = 0$). Current networking architectures for large LEO constellations consider the presence of four satellite first-neighbor connections, among which two are established with satellites in the same orbital plane (drawn in black) and the other two with satellites in adjacent planes (drawn in red).

of connection. In order not to load the notation too much, we are denoting the norm of the relative position vector, $\|r\|$ simply by r where the context is clear. FSPL can be promptly estimated from link length using

$$L = \left(\frac{\lambda_c}{4\pi\|r\|}\right)^2, \qquad (2)$$

where $\lambda_c = 1550$ nm is the carrier wavelength [23].

Intraorbital connections are not influenced by system dynamics in the Walker's circular orbits approximation. This time invariance allows them to be easily evaluated using the law of cosines:

$$\bar{r} = \sqrt{2R^2\left[1 - \cos\left(\frac{2\pi}{S}\right)\right]}. \qquad (3)$$

Interorbital connections, on the other hand, have lengths that vary with a period T_{ISL} corresponding to half the satellites' orbital period T. Mathematically,

$$T_{ISL} = \frac{T}{2} = \pi\sqrt{\frac{R^3}{GM_\oplus}}, \qquad (4)$$

where $G \approx 6.6743 \times 10^{-11}$ m^3 kg^{-1} s^{-2} is the gravitational constant and $M_\oplus \approx 5,972 \times 10^{24}$ kg is the Eath mass [24]. For this scenario, the results were numerically assessed, with a time resolution taken as 1 ms for the orbit simulation.

The longest link lengths exhibited by interorbital first-neighbor connections for the considered architectures are both in the C$^{(4)}$ shell, with $9,801.91$ km (k-to-k) and $9,921.22$ km (k-to-$k-1$), representing an FSPL of 278 and 278.11 dB, respectively. In interobital connections, the longest distance between first neighbors is in charge of the A$^{(1)}$ shell, with $3,535.17$ km, which reflects in an FSPL of 269.15 dB, as a result of the combination of relatively high orbits and few

satellites per plane. From the point of view of the closest approach between the terminals, A$^{(1)}$ reaches 5.01 km, with a corresponding FSPL of 212.17 dB, in the k-to-k case, while D$^{(1)}$ promotes an approach of only 620 m, with attenuation by FSPL of 193.98 dB, for k-to-$k-1$. In terms of intraorbital connections, B$^{(2)}$ and B$^{(3)}$ shells reach the minimum distances among all configurations with 660.58 km, and FSPL of 254.57 dB, since both shells have the same altitude and the same number of satellites per orbital plane.

As concerns the phase factors, it is possible to notice that, in general, the extreme values of this parameter, i.e. $F = 0$ and $F = P - 1$, are those that most commonly take the links to their maximum and minimum length values, although there are important exceptions (e.g., A$^{(1)}$ and several shells of the constellation C). Furthermore, given the differences in link altitude promoted by the change in the phase factor, and in view of the relatively small link length excursion in most cases, it is possible to observe that, in all shells, $\hat{F}_{min} \neq \hat{F}_{max}$ and $\tilde{F}_{min} \neq \tilde{F}_{max}$. In certain shells – such as A$^{(1)}$, A$^{(2)}$, C$^{(1)}$, and C$^{(2)}$ – patterns like $\hat{F}_{min} = \tilde{F}_{max}$ or $\tilde{F}_{min} = \hat{F}_{max}$ can be observed as a direct consequence of the fact that the k-to-$k-1$-type connections are essentially k-to-k connections with an added phase factor that results in an angular inter-plane offset equal to $2\pi/S$ rad. It should be pointed out that certain values of the phase factors can cause collisions between satellites, other than first neighbors, within the same shell [25], [26]; this discussion, however, is beyond the scope of this study.

Link preservation, even in first-neighbor connections, can be compromised both by the occlusion of the beam by the Earth's surface and by atmospheric factors as it leaves the thermosphere. Bhattacherjee and Singla [27] stress the importance of ISLs staying at least 80 km from the Earth's surface in order to avoid constraints associated with visibility or even attenuation

TABLE II

MAXIMUM AND MINIMUM VALUES FOR THE FSPL AND THE RESPECTIVE RELATIVE DISTANCES IN FIRST-NEIGHBOR INTRA AND INTERORBITAL CONNECTIONS BASED ON THE WCM FOR COMMERCIAL CONSTELLATIONS. $\mathbf{F}_{\mathrm{MAX}}$ ($\mathbf{F}_{\mathrm{MIN}}$) IS THE VALUE OF THE PHASE FACTOR THAT RESULTS IS THE MAXIMUM (MINIMUM) LINK LENGTH, FOR k-TO-k AND k-TO-$k-1$-TYPE CONNECTION GIVEN THE OTHER PARAMETERS OF THE CONSTELLATION. TEXT COLORS INDICATE THE LOWEST ATMOSPHERIC LAYER REACHED BY THE OISL: IN VIOLET ARE THE LINKS THAT REMAIN IN THE EXOSPHERE, IN BLUE, THOSE THAT REACH THE THERMOSPHERE, AND IN RED, THOSE THAT, AT A CERTAIN MOMENT, UNDERGO EARTH-OCCLUDED.

	Intraorbit	k-to-k Interorbit		k-to-$k-1$ Interorbit	
Shell	$\bar{L}$ [dB] ($\bar{r}$ [km])	$\hat{L}_{\min}$ [dB] ($\hat{r}_{\min}$ [km]) $\left[\hat{\boldsymbol{F}}_{\min}\right]$	$\hat{L}_{\max}$ [dB] ($\hat{r}_{\max}$ [km]) $\left[\hat{\boldsymbol{F}}_{\max}\right]$	$\tilde{L}_{\min}$ [dB] ($\tilde{r}_{\min}$ [km]) $\left[\tilde{\boldsymbol{F}}_{\min}\right]$	$\tilde{L}_{\max}$ [dB] ($\tilde{r}_{\max}$ [km]) $\left[\tilde{\boldsymbol{F}}_{\max}\right]$
$A^{(1)}$	269.15 (3,535.17)	212.17 (5.01) [2]	262.78 (3,552.94) [26]	250.20 (398.99) [26]	270,50 (4,134.13) [0]
$A^{(2)}$	261.48 (1,463.10)	255.82 (761.96) [0]	265.69 (2,373.65) [39]	213.13 (5.59) [19]	259.65 (1,184.94) [39]
$B^{(1)}$	257.91 (970.15)	231.87 (48.36) [0]	262.52 (1,647.81) [35]	212.78 (5.37) [34]	262.30 (1,606.98) [0]
$B^{(2)}$	254.57 (660.48)	256.78 (851.29) [0]	263.85 (1,921.00) [31]	243.90 (193.17) [0]	261.54 (1,472.49) [31]
$B^{(3)}$	254.57 (660.48)	259.29 (1,136.94) [0]	264.25 (2,013.11) [31]	251.78 (478.56) [0]	261.51 (1,468.49) [31]
$C^{(1)}$	264.05 (1,967.07)	249.33 (361.16) [0]	265.58 (2,345.88) [71]	212.22 (5.04) [59]	262.68 (1,678.64) [0]
$C^{(2)}$	264.07 (1969.92)	249.38 (363.36) [0]	265.60 (2,350.65) [71]	214.74 (6.73) [59]	262.68 (1,679.11) [0]
$C^{(3)}$	255.68 (750.47)	249.64 (374.05) [5]	274.99 (6,931.00) [0]	258.39 (1,025.00) [5]	275.14 (7,046.17) [0]
$C^{(4)}$	258.28 (1011.86)	255.77 (757.59) [3]	278.00 (9,801.91) [0]	261.55 (1,475.17) [3]	278.11 (9,921.22) [0]
$C^{(5)}$	264.91 (2171.62)	250.51 (413.81) [0]	266.99 (2,757.98) [35]	216.97 (8.71) [29]	264.58 (2,090.79) [0]
$D^{(1)}$	262.03 (1558.77)	260.50 (1,307.29) [0]	267.48 (2,919.67) [27]	226.86 (27.17) [4]	261.77 (1,512.57) [27]
$D^{(2)}$	259.88 (1216.86)	257.30 (904.31) [0]	265.16 (2,233.42) [35]	215.46 (7.31) [9]	259.70 (1,192.02) [35]
$D^{(3)}$	260.40 (1,291.94)	256.21 (797.17) [0]	265.34 (2,281.69) [33]	193.98 (0.62) [13]	260.25 (1,268.91) [33]

of the beam's power by water vapor present in the mesosphere. The greater the distance between a pair of connected satellites, the greater the probability that the beam will occlude, or that it will reach atmospheric layers that promote its degradation, as is the case of the mesosphere, stratosphere, and troposphere. Ideally, OISLs should remain in the thermosphere (which starts at approximately 80 km above sea level) or in the exosphere. Among the considered architectures, only the $C^{(3)}$ and $C^{(4)}$ shells are Earth-occluded. The three main features responsible for this behavior are the small number of orbital planes (6 and 4, respectively), the high inclination, and the low altitude. It must be noted that other polar shells, such as $A^{(1)}$ and $B^{(1)}$, for example, do not even reach the thermosphere. The dwell time of the beam in each atmospheric layer assuming worst-case scenarios ($\hat{F}_{max} = \tilde{F}_{max} = 0$) for **C** polar shells is shown in Fig. 3. Considering the orbital period of the satellites in $C^{(3)}$ ($T \approx 5,740$ s), we have that the link remains above the mesosphere, i.e. in the ISL-friendly region, for approximately

$2,800$ s, which is about half the orbital period, whereas for $C^{(4)}$, with two less orbital planes than $C^{(3)}$ and the same T, this value reduces to about 30% of the orbital period.

V. CONCLUSION

In this work we present the typical values of link lengths in first-neighbor inter-satellite optical connections for ultra-dense next-generation LEO constellations, taking into account intra and interorbital connections. For all constellations and topologies studied, the values of the phase factor that maximize and minimize the link length were established, contributing to delineating the worst and best case scenarios in connections with first neighbors. The corresponding values for the attenuation, resulting from the beam's geometric scattering, were also computed. It has been found that, in general, k-to-k-type interorbital connections in polar orbits tend to promote a smaller distance between the transmitter and receiver satellites compared to those of the k-to-$k-1$-type – a feature that is

(a) k-to-k connection in the $C^{(3)}$ shell.

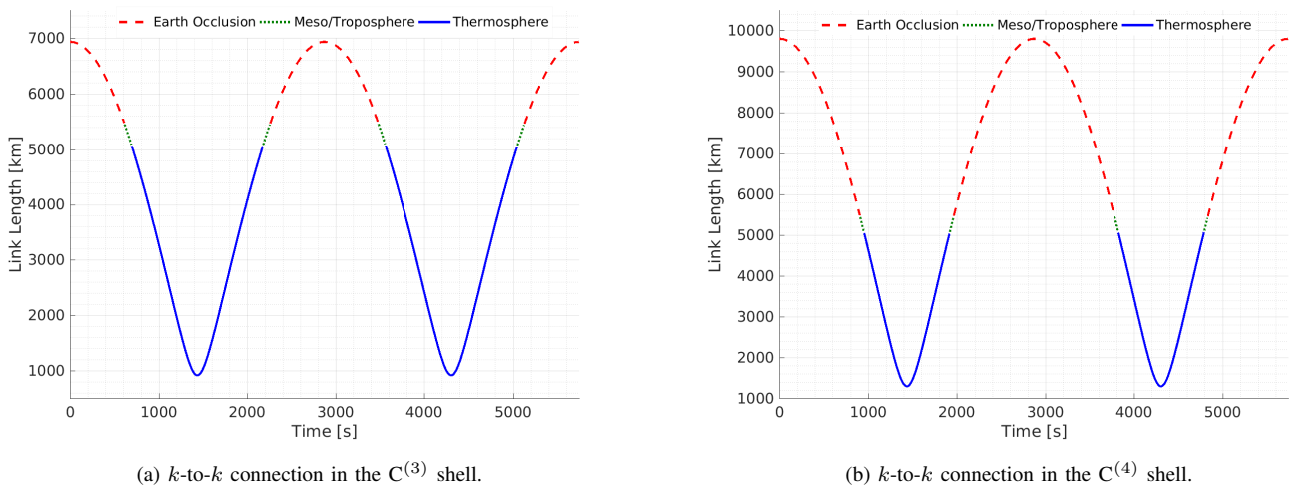(b) k-to-k connection in the $C^{(4)}$ shell.

Fig. 3.   First-neighbor OISLs distance in $C^{(3)}$ and $C^{(4)}$ shells. The distinct colors in each curve indicate the time the link remains in each atmospheric layer or the occurrence of Earth occlusion.

not maintained when considering medium-inclination orbits. At last, the minimum altitude of the links was categorized according to the atmospheric layers crossed by them over an orbital period, highlighting eventual Earth's occlusion or changes in the physical conditions of the propagation medium. Based on the Walker model, only two of the thirteen evaluated architectures exhibited issues related to occlusion of the beam.

REFERENCES

[1] S. Finkelstein and S. H. Sanford, "Learning from corporate mistakes: The rise and fall of Iridium," *Organizational Dynamics*, v. 29, n. 2, p. 138-148, 2000.

[2] C. Christensen and S. Beard, "Iridium: failures & successes," *Acta Astronautica*, v. 48, n. 5-12, p. 817-825, 2001.

[3] I. del Portillo, B. G. Cameron, and E. F. Crawley, "A technical comparison of three low Earth orbit satellite constellation systems to provide global broadband," *Acta Astronautica*, 2019.

[4] N. Pachler, I. del Portillo, E. F. Crawley, and B. G. Cameron, "An updated comparison of four low Earth orbit satellite constellation systems to provide global broadband," *2021 IEEE international conference on communications workshops (ICC workshops)*. IEEE, 2021. p. 1-7.

[5] Y. Ulybyshev, "Satellite constellation design for complex coverage," *Journal of Spacecraft and Rockets*, v. 45, n. 4, p. 843-849, 2008.

[6] V. L. Foreman, A. Siddiqi, O. De Weck, "Large satellite constellation orbital debris impacts: Case studies of OneWeb and SpaceX proposals," *AIAA SPACE and Astronautics Forum and Exposition*, p. 5200, 2017.

[7] J. Radtke, C. Kebschull, E. Stoll, "Interactions of the space debris environment with mega constellations—Using the example of the OneWeb constellation," *Acta Astronautica*, v. 131, p. 55-68, 2017.

[8] S. Le May, S. Gehly, B. A. Carter, and S. Flegel, "Space debris collision probability analysis for proposed global broadband constellations," *Acta Astronautica*, v. 151, p. 445-455, 2018.

[9] C. McLain and J. King, "Future Ku-band mobility satellites," *Proceedings of the 35th AIAA International Communications Satellite Systems Conference*, 2017, p. 5412.

[10] T. G. Reid, A. M. Neish, T. Walter, and P. K. Enge, "Broadband LEO constellations for navigation," *Navigation: Journal of The Institute of Navigation*, vol. 65, no. 2, pp. 205–220, 2018.

[11] Telesat Canada. (2016) SAT-PDR-20161115-00108. [Online]. Available: http://licensing.fcc.gov/myibfs/forwardtopublictabaction.do?filenumber=SATPDR2016111500108.

[12] Telesat Canada. (2020) SAT-MPL-20200526-00053. [Online]. Available: http://licensing.fcc.gov/myibfs/forwardtopublictabaction.do?filenumber=SATMPL2020052600053.

[13] WorldVu Satellites Limited. (2016) SAT-LOI-20160428-00041. [Online]. Available: http://licensing.fcc.gov/myibfs/forwardtopublictabaction.do?filenumber=SATLOI2016042800041.

[14] WorldVu Satellites Limited. (2020) SAT-MPL-20200526-00062. [Online]. Available: http://licensing.fcc.gov/myibfs/forwardtopublictabaction.do?filenumber=SATMPL2020052600062.

[15] WorldVu Satellites Limited. (2021) SAT-MPL-20210112-00007. [Online]. Available: http://licensing.fcc.gov/myibfs/forwardtopublictabaction.do?filenumber=SATMPL2021011200007.

[16] Space Exploration Holdings, LLC. (2016) SAT-LOA-20161115-00118. [Online]. Available: http://licensing.fcc.gov/myibfs/forwardtopublictabaction.do?filenumber=SATLOA2016111500118.

[17] Space Exploration Holdings, LLC. (2018) SAT-MOD-20181108-00083. [Online]. Available: http://licensing.fcc.gov/myibfs/forwardtopublictabaction.do?filenumber=SATMOD2018110800083.

[18] Space Exploration Holdings, LLC. (2019) SAT-MOD-20190830-00087. [Online]. Available: http://licensing.fcc.gov/myibfs/forwardtopublictabaction.do?filenumber=SATMOD2019083000087.

[19] Space Exploration Holdings, LLC. (2020) SAT-MOD-20200417-00037. [Online]. Available: http://licensing.fcc.gov/myibfs/forwardtopublictabaction.do?filenumber=SATMOD2020041700037.

[20] SpaceX Services, Inc. (2020) SES-LIC-20201023-01173. [Online]. Available: http://licensing.fcc.gov/myibfs/forwardtopublictabaction.do?filenumber=SESLIC2020102301173.

[21] Kuiper Systems LLC. (2019) SAT-LOA-20190704-00057. [Online]. Available: http://licensing.fcc.gov/myibfs/forwardtopublictabaction.do?filenumber=SATLOA2019070400057.

[22] J. G. Walker, "Some circular orbit patterns providing continuous whole earth coverage," *Journal of the British Interplanetary Society*, v. 24, p. 369-384, 1971.

[23] H. Hemmati, *Near-earth laser communications*. CRC Press, 2020.

[24] V. A. Chobotov, *Orbital mechanics*. American Institute of Aeronautics and Astronautics (AIAA), 2002.

[25] M. Handley, "Delay is not an option: Low latency routing in space," *Proceedings of the 17th ACM Workshop on Hot Topics in Networks*, pp. 85–91, 2018.

[26] J. Liang, A. U. Chaudhry, and H. Yanikomeroglu. "Phasing parameter analysis for satellite collision avoidance in Starlink and Kuiper constellations," *Proceedings of the 2021 IEEE 4th 5G World Forum (5GWF)*, IEEE, p. 493-498, 2021.

[27] D. Bhattacherjee and A. Singla, "Network topology design at 27,000 km/hour," *Proceedings of the 15th International Conference on Emerging Networking Experiments And Technologies*, 2019.